REPORT DOCUMENTATION PAGE

Form Approved OMB No. 0704-0188

1. REPORT DATE *(DD-MM-YYYY)*	2. REPORT TYPE	3. DATES COVERED *(From – To)*
30-05-2002	Final Report	3 August 2001 - 30-Jul-02

4. TITLE AND SUBTITLE

Polar Cap Dynamics and Formation of High-Latitude Ionospheric Irregularities

5a. CONTRACT NUMBER
F61775-01-WE051

5b. GRANT NUMBER

5c. PROGRAM ELEMENT NUMBER

6. AUTHOR(S)

Professor Jøran Moen

5d. PROJECT NUMBER

5d. TASK NUMBER

5e. WORK UNIT NUMBER

7. PERFORMING ORGANIZATION NAME(S) AND ADDRESS(ES)

University of Oslo
Box 1048 Blindern
N-0316 Oslo
Norway

8. PERFORMING ORGANIZATION REPORT NUMBER

N/A

9. SPONSORING/MONITORING AGENCY NAME(S) AND ADDRESS(ES)

EOARD
PSC 802 BOX 14
FPO 09499-0014

10. SPONSOR/MONITOR'S ACRONYM(S)

11. SPONSOR/MONITOR'S REPORT NUMBER(S)
SPC 01-4051

12. DISTRIBUTION/AVAILABILITY STATEMENT

Approved for public release; distribution is unlimited.

13. SUPPLEMENTARY NOTES

14. ABSTRACT

This report results from a contract tasking University of Oslo as follows: The contractor will investigate disturbances in the polar ionosphere caused by fluctuating solar winds. In particular, he will attempt to accurately locate the boundary between open and closed magnetic field lines and then determine which processes occur on each of the field lines. These measurements will be made during quiet and disturbed conditions. The final report will contain an analysis of these measurements.

15. SUBJECT TERMS
EOARD, Electromagnetics, Ionosphere, Atmospheric Propagation

16. SECURITY CLASSIFICATION OF:			17. LIMITATION OF ABSTRACT	18, NUMBER OF PAGES	19a. NAME OF RESPONSIBLE PERSON
a. REPORT	b. ABSTRACT	c. THIS PAGE			David M. Burns, Lt Col, USAF
UNCLAS	UNCLAS	UNCLAS	UL	27	**19b. TELEPHONE NUMBER** *(Include area code)* +44 (0)20 7514 4955

SPC: 01-4051
Contract number: F61775-01-WE051

FINAL REPORT

on

Polar Cap Dynamics and Formation of High-Latitude Ionospheric Irregularities

by

Professor Jøran Moen, PI
Professor Alv Egeland, Co-I

24 May, 2002

Correspondence to:
Prof. Jøran Moen
Department of Physics
P.O. Box 1048, Blindern
N-0316 Oslo, Norway
e-mail: jmoen@fys.uio.no

1. Technical support on the AFRL scintillation receivers on Svalbard

Dr. Santimay Basu and his engineers installed a new scintillation receiver at Longyearbyen (78.92^0N, 11.95^0E, 76.07 CGMLat), and upgraded the existing system at Ny-Ålesund (78.20^0N, 15.82^0E, 75.12 CGMLat). The technical assistance from the University of Oslo (UiO) comprised logistics, obtaining the necessary permissions, and to provide internet connection for the two set of equipment. The instrument at Ny-Ålesund is networked via UNINETT (governmental network for the Norwegian universities), and via a dedicated telephone line during campaigns when demands on transfer rate are higher. The Longyearbyen and the Ny-Ålesund receivers have both been in continuous operation since the end of August 2001, and provide unique stereo observations of irregularities in the vicinity of the auroral oval. Both receivers will be operated remotely and data will be transferred to AFRL via our network.

2. Observation campaigns

We assisted AFRL researchers in conducting three intensive observing campaigns: 6-21 December, 2001; 9-21 January, 2002; and 6-10 February, 2002. During all these campaigns UiO complemented the scintillation experiment with optical recordings at Ny-Ålesund. During the December 2001 and February 2002 campaigns we operated special program modes at the EISCAT Svalbard radar, as well as EISCAT UHF and the VHF systems at Tromsø, and we arranged CUTLASS HF radar support via University of Leicester.

DECEMBER 2001:
In December 2001 we carried out an extensive campaign to monitor the formation of ionospheric patches near the cusp inflow region. In addition to the EISCAT Svalbard Radar we used the EISCAT Tromsø UHF and VHF systems to map the polar cap boundary and the general flow pattern. The Tromsø VHF was operated in a split-beam V-configuration at 30 degree elevation over Svalbard (lowest possible). The Tromsø UHF, which is moveable both in azimuth and elevation) was operated at different scan modes A-E:

EISCAT UHF Mode specification:
30 sec dwell and 10 sec motion (first 10 s of every 40 s is moving)
Mode A: El 21.5; Az 7.5, 15, 22.5, 30, 22.5, 15, 22.5, 15 (2 min half cycle)
Mode B: El 21.5; Az 330, 337.5, 345, 352.5, 360, 7.5, 15, 7.5, 360, 352.5, 345, 337.5 (4 min half cycle)
Mode C: El 21.5; Az 337.5, 345.5, 352.5, 360, 352.5, 345 (2 min half cycle)
Mode D: Az 360; El 21.5, 23.5, 21.5, 25.5, 21.5 (2 min half cycle)
Mode E: Az 315, 322.5, 330, 337.5, 330, 322.5 (2 min half cycle)

The movable antenna of Eiscat Svalbard Radar (ESR-1) was operated in a set of windshield modes to sweep larger sectors (90-120 degrees in azimuth) including the anticipated cusp location. The aim was to map patch formation near the cusp inflow region and to map dimension and movement of ionospheric patches. The different modes prepared for this campaign is given below. The Mode 02-MSP scanned in the same plane as the meridian

scanning photometers at Ny-Ålesund and Longyearbyen, and hence provides a simple geometry for comparison of optical cusp dynamics and patch formation:

ESR-1 Mode specification:
Mode 01-90 E: El 30; Az 15-105 (128s half cycle)
Mode 02-MSP: Az 45, El 30-150 (128s half cycle)
Mode 03-90 W: El 150; Az 15-105 (128s half cycle)
Mode 04-90 N: El 30; Az (-75)-15 (128s half cycle)
Mode 05-90 S: El 30; Az 105-195 (128s half cycle)
Mode 06-120 E: El 30; Az 0-120 (192s half cycle)
Mode 07-120 W: El 150; Az 0-120 (192s half cycle)
Mode 08-120 N: El 30; Az (-60)-60 (192s half cycle)
Mode 09-120 S: El 30; Az 90-210 (192s half cycle)
Mode 10-360 N: El 150; Az (-225)-135 (512s half cycle)
Mode 11-120 N + vertical (ESR-2): El 30; Az (-60)-60 (384s half cycle)

See Appendix A for a detailed campaign notes, in which start and stop times for the different experiment modes are given as well as brief comments are given on auroral observing conditions, and events of particular interest are highlighted etc.

JANUARY 2002:
In January we supported the scintillation experiment by our optical instrumentation at Ny-Ålesund. This campaign was not supported by EISCAT special program time. See Appendix B for observing conditions and data coverage.

FEBRUARY 2002:
In February 2002 and conducted an extensive campaign to monitor plasma patches exiting the polar cap at the nightside. Again we operated Tromsø VHF in a split-beam V-configuration at 30 degree elevation over Svalbard (lowest possible) and the Tromsø UHF was operated in two different beam-swing modes:

EISCAT UHF Mode description:
30 sec dwell and 10 sec motion (first 10 s of every 40 s is moving)
Mode West: A: El 21.5; Az 330, 315, 300, 285, 300, 315 (4 min cycle)
Mode East: El 21.5; Az 15, 30, 45, 60, 45, 30 (4 min cycle)

The ESR-1 was operated at fast windshield modes for tracking patches as well monitoring their dimension and shape:

ESR-1 Mode description:
Mode East: El. 30: Az (-30)-160 windshield (3minutes-192 s/ 4 minutes-256s)
Mode West: El. 150: Az (-30)-160 windshield (3minutes-192 s/ 4 minutes-256s)
Mode North: El. 30: Az (-90)-90 Windshield (3 minutes -192 s)
Mode 4 from Jan 2001: az = [-75,15], el = 30 (P = 2 min (256s) cycle time)

See Appendix C for a detailed campaign notes, in which start and stop times for the different experiment modes are given as well as brief comments are given on auroral observing conditions, and events of particular interest are highlighted etc.

3. Scientific results

Svalbard is ideally located to carry out experimental studies on ionopsheric irregularities near the cusp. We have carried out one project to investigate small-scale cusp irregularities observed as strong backscatter echoes by the network of SuperDARN radars, and combined that with optical observations of the cusp aurora. Furthermore we have studied the plasma gradient associated with HF cusp backscatter. This in order to test the hypothesis that the gradient drift instability plays a dominant role for generating HF backscatter targets.

3.1 On the collocation between cusp auroral emission and HF-radar backscatter

All-sky cameras and SuperDARN HF radars with large fields of view constitute powerful tools to study temporal and spatial behaviour of large-scale auroral and polar cap dynamics, and both techniques have proven potential for identification of magnetospheric boundary layers. Several attempts have been made to compare HF radar and optical cusp observations. Rodger *et al.* (1995) employed wide spectral widths as a radar cusp identifier. For the situation when IMF Bz was documented negative, they found the equatorward boundary of the HF cusp signature to be located 0.5^0 on average equatorward of the optical cusp. For the other case of unknown IMF conditions, the radar cusp boundary was either embedded within or located near the poleward edge of the auroral luminosity. Yeoman *et al.* (1997) demonstrated a near collocation of strong HF backscatter power, poleward moving auroral forms, and energy dispersed ions for a DMSP snapshot through the winter cusp above Svalbard. Milan *et al.* (1999) demonstrated a good correlation between CUTLASS HF backscatter and dayside 630.0 nm aurora along the meridian swept by the scanning photometer at Ny-Ålesund, Svalbard. They found a rather good collocation of the equatorward radar (defined by power) and optical cusp auroral boundaries, and that these boundaries showed the same motion.

The motivation for our study was to follow up on Rodger *et al.* (1995) and Baker *et al.* (1995) to validate use of enhanced radar Doppler spectral widths as a cusp identifier around magnetic noon for one specific category of cusp aurora. The work was limited to Type 1 cusp auroral activity. According to the classification by Sandholt *et al.* (1998), Type 1 cusp aurora occur under predominantly southward IMF conditions, located typically south of $\sim 74^0$ MLAT, includes quasi-periodic sequences of poleward moving auroral forms (PMAFs), and is dominated by the 630.0 nm emission which indicates soft magnetosheath electron precipitation. The pattern of east-west movements of Type 1 cusp activity is IMF B_Y controlled (e.g. Sandholt *et al.* 1993; Moen *et al.*, 1999). Moen *et al.* (1996) attributed the equatorward boundary of the Type 1 aurora to an open LLBL, located poleward of the electron-trapping boundary. Sandholt *et al.* (1993) attributed the fading phase of a poleward moving Type 1 auroral form to approaching the plasma mantle. LLBL, cusp and mantle precipitation regimes can be separated from each other based on differential ion energy fluxes (Newell *et al.*, 1988), but are indistinguishable in an electron stimulated auroral display (e.g. Moen *et al*, 1998). Type 1 cusp aurora is interpreted as LLBL stimulated reconnection and is taken to be the auroral footprint of newly-opened magnetic flux. The transition from narrow single component to wide complex Doppler spectra of coherent HF backscatter has been proposed as a delineator of the open/closed field line boundary (Baker *et al*, 1995). Hence, it

is reasonable to expect a good correlation between the equatorward boundaries of radar and optical auroras for Type 1 cusp activity.

This is demonstrated in Figure 1 showing a sequence of all-sky images from 0920 to 0950 UT (~10 min intervals) on December 17, 1995. The colour scale is linear with increasing intensity from blue to red. The yellow squares superimposed onto the all-sky images mark position of the radar gates with spectral width ≥220 ms^{-1}. Backscatter with insufficient signal to noise ratio were discarded when employing the spectral width filtering on the data. This cut-off was taken to be the 0 dB at lag 0 in the ACF. All-sky imagery reveals that the equatorward edge of the cusp aurora lines up with the equatorward edge of the HF backscatter boundary. The 630.0 nm and spectral width boundaries are notably very similar in shape, even when the boundary is undulating or changing, so it appears to be an intimate relationship between the optical cusp boundary and the HF radar cusp backscatter boundary.

In the top panel of Figure 2 the southernmost gate position of spectral widths ≥220 m/s has been plotted as a function of the 630.0 nm auroral boundary obtained by the meridian scanning photometer (MSP). The plot includes only the periods of a well-established radar cusp boundary within the MSP field of view from 09-10 UT on December 17, 1995 and from 0920 and 1010 UT on December 24, 1995. For physical reasons explained by Moen et al. (2001) the emission altitude was assumed to be 220 km on the December 17 and 250 km on December 24. The boundary motions for December 17 and 24 are clustered around 71 and 73.5 CGMLAT, respectively. On both days the auroral activity was situated south of the MSP observation site located at 76 CGMLAT. The full line depicts a least-square fit representation of the two data sets, and the dashed line serves as a guideline to co-location of the two boundaries. The large spread of data points (±1 degree latitude = ± 110 km) about the best fit line seem to worsen with latitude, if there is any latitude dependence to be found. If the spread were due to a time varying emission altitude of the 630.0 nm

emission, the spread would have diminished towards the MSP site of 76 CGMLAT. A random variation in emission altitude between 215-250 km would introduce a scatter in auroral boundary location of ~0.7 degrees around 70.5 CGMLAT (5 degrees in latitude south of Ny-Ålesund) and ~0.4 degrees around 73.5 CGMLAT (2.5 degrees in latitude south of Ny-Ålesund). The quite opposite trend in latitude spread around the best fit lines in Figure 2 indicates that the spread is rather being introduced by the physical nature of radar cusp backscatter/ radio wave propagation, e.g.:

i) Uncertainty in the geographic location of the radar echoes.
ii) The 220 ms^{-1} criterion used for the radar cusp boundary.
iii) The generation mechanism of plasma irregularities.

Point i) is related to the fact that we do not know the exact radio wave propagation path. Range determination performed by the radars is based on the time-of-flight of radar returns. This provides an accurate measure of the length of the group path taken by the radar signal (also known as slant range or radar range), but this is an overestimate of the ground range to the scatter volume. A detailed knowledge of the electron density distribution within the radar's propagation environment would allow a ray-tracing analysis to transform from radar

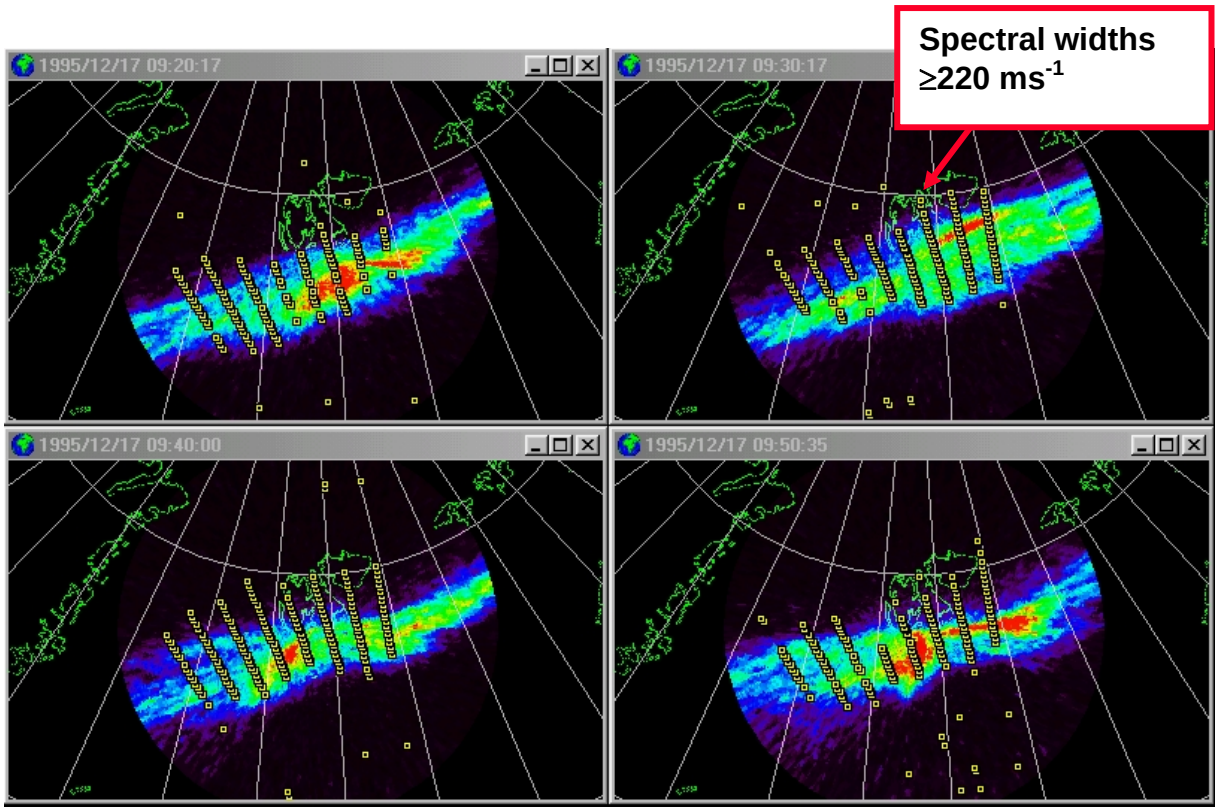

Figure 1: A selection of 4 colour-coded (ranging from blue to red with increasing intensity) all-sky images of the 630.0 nm aurora for the period 0920.17 UT to 0950.35 UT on December 17, 1995. The auroral emission is mapped onto a geographical grid assuming an emission altitude of 215 km. The images have been cut at 75^0 zenith angle. The yellow squares mark positions of gates with spectral widths ≥220ms^{-1} along CUTLASS Finland beams 5-11 from west to east.

range to ground range accurately. Without this detailed knowledge, however, assumptions must be made regarding the characteristics of the propagation mode to the scatter volume. Such considerations, specifically whether radar signals propagate by the 0.5-F mode or 1.5-F mode, have been discussed at some length by Milan *et al.* (1997, 1998): near- and far-range scatter is expected to propagate by the 0.5-F and 1.5-F modes, respectively. For simplicity our analysis of SuperDARN data assumes that all echoes are 0.5-F mode returns, that signals propagate at the speed of light in vacuo, and that the ray path is a straight line, that is the effect of refraction is neglected. These assumptions tend to overestimate the range to more distant scatter if a realistic scattering altitude (~250 km) is used in the calculations, so to overcome this we further assume that the scatter originates from the artificially high altitude of 400 km. This compromise is found to work well for most ranges, though the inaccuracy increases with greater distance. The accuracy of our range determination can be tested with the Tromsø high power radio wave facility which artificially stimulates ionospheric irregularities at a known altitude and location from which the CUTLASS radars receive coherent backscatter (see for instance Wright and Yeoman, 1999). At a range of 2000 km, the assumptions employed in the routine analysis discussed above lead to a systematic overestimate in the range to the heater volume of some 60 km (T. K. Yeoman, personal communication, 2000). This represents the first and only direct measurement of absolute range by a SuperDARN radar, but other studies have investigated the range accuracy between different propagation modes. These include: Milan *et al.* (1998) who examined a case in which propagation to the dayside auroral zone changed sharply between the 0.5-F and 1.5-F mode with little discernable change in range being observed; André *et al.* (1997) who

compared observations at different radar operating frequencies and demonstrated a range consistency of the order of 45 km or one standard range gate; and modelling work by Villain *et al*. (1985) which again estimated that range uncertainty was of the order of 45 km or less.

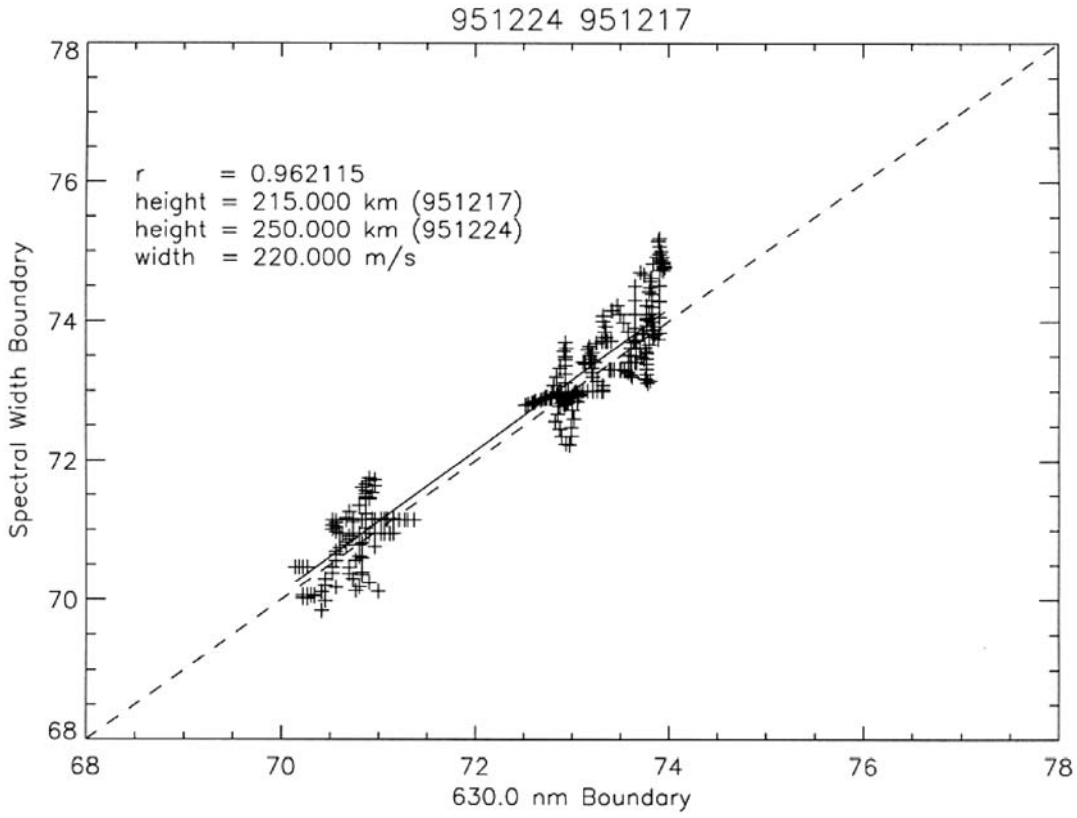

Figure 2: The location of the equatorward edge of the 630.0 nm cusp and CUTLASS HF radar cusp for 09-10 UT on December 17 and 0920-1020 UT on December 24, 1997. The full line in each diagram represent the least square fit to both data sets, and the broken line serve as a guideline for radar and 630.0 nm boundary co-location. See text for more details.

Our overall conclusion is that for the distances of interest in the present study the range uncertainty due to the radar data analysis is no larger than 60 km (corresponding to four 15 km gates on December 17 and two 30 km range gates on December 24) and that this is likely to be an overestimate of the true range. Furthermore, for each event this overestimate will be systematic, that is the equatorward boundary of cusp backscatter, which is of particular interest for this study, will be displaced in latitude but its shape should remain essentially unchanged. We note in fact from Figure 2 that the 630.0 nm and spectral width boundaries are very similar in shape, even when the boundary is undulating or changing. Thus, uncertainties in mapping the slant range to geographic location are expected to shift the boundary location by ~40-60 km, but are not expected to cause scatter of ± 1 degree as is the case in Figure 2. Hence, we suggest that this spread is caused mainly by Points ii) and iii)

3.2 On the formation of cusp backscatter irregularities

Coherent HF radars obtain backscatter echoes from field-aligned plasma irregularities of decametre scale length (½ the radar operating wavelength). The generation mechanism of backscatter targets has not yet been agreed upon, but the literature has identified candidate

processes including: gradient drift instability, shear instability, "stirring" or flux tube interchange, and current convective instability. The latter can be viewed as a subset of gradient drift instabilities (e.g. Tsunoda, 1988; Basu *et al.*, 1994). Under conditions for which plasma flow has a component in the direction of a density gradient, gradient drift instability is regarded as the dominant mode for driving the plasma unstable in the F-region auroral ionosphere (e.g. Ossakow and Chaturvedi, 1979; Basu *et al.*, 1994). The typical geometry for gradient drift instabilities in the Northern Hemisphere cusp, is a density gradient towards north, a convection electric field pointing eastward and a background magnetic field pointing down. Notable is that the **E**x**B** gradient drift geometry will become stable upon reversing the electric field or the density gradient. Moen *et al*. (2001) observed an abrupt fade in radar cusp backscatter connected to an IMF B_Z polarity change found consistent with switching the gradient drift instability from an unstable (on) to a stable geometry (off).

Moen et al. (2002) carried out an attempt to test the role of gradient drift instability as a generation mechanism for plasma irregularities in the cusp. Their observations are summarised in Figure 3. The right-hand panel shows the 630.0 nm all-sky image taken at Ny-Ålesund at 0836.31 UT on January 14, 2000. The line superimposed depicts the orientation of the plane of the radio tomographic image presented in the left panel, which we will be described soon. Also superimposed are observations from the CUTLASS radar in Finland. The radar operated in a mode scanning counter-clockwise (east to west) from beam 15 to beam 0, with each scan starting on the minute and lasting 52 s. Data from the scan commencing 0834 UT have been filtered to include only those for which the spectral width was $\geq 220 ms^{-1}$, the criterion identified earlier for cusp backscatter. Yellow squares mark the centre positions of the corresponding range gates. Figure 3 demonstrates clearly that the equatorward edge of the spectral-width boundary aligns closely with the ragged equatorward boundary of the optical cusp. In the vicinity of the NIMS observation plane, both boundaries lie at about 73.5^0N, corresponding to about 70.7^0N CGMLAT.

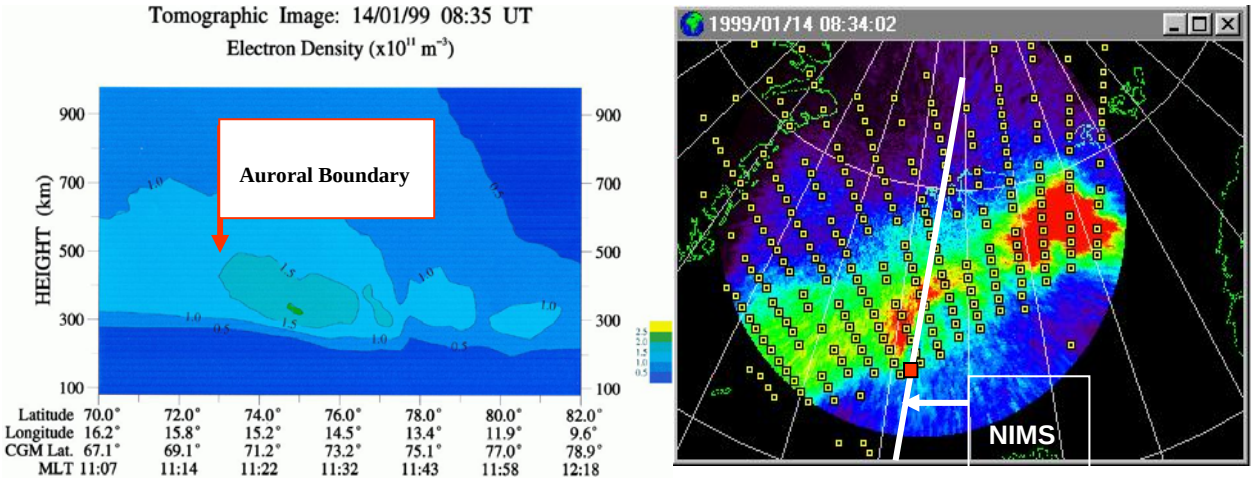

Figure 3 (Left panel) Tomographic image of electron density obtained from a NIMS satellite that traversed the auroral cusp from north to south as indicated by the white line and crossed 75^0N at 0835 UT. The red arrow marks the equatorward limit of the 630.0 nm emission boundary. (Right panel) The 630.0 nm all-sky image taken at 08:34 UT has been projected on to a geographic frame of reference assuming an emission height of 250 km. Emission intensity is colour-coded from blue to red with increasing intensity. The red square in the NIMS satellite track corresponds to the arrow in the left panel, and the yellow squares mark the position of CUTLASS radar gates identified with cusp backscatter.

The radio tomography monitoring system comprises receivers at Ny-Ålesund (78.9^{0}N, 12.0^{0}E), Longyearbyen (78.2^{0}N, 15.3^{0}E), Bjørnøya (74.5^{0}N, 19.0^{0}E) and Tromsø (69.8^{0}N, 19.0^{0}E). Measurements are made of ionospheric total electron content using signals from satellites in the NIMS (Navy Ionospheric Monitoring System) constellation. The observations are then inverted in a reconstruction algorithm to create spatial images of electron density as a function of height and latitude, with a horizontal resolution of about 25 km. The left panel of Figure 3 shows the tomographic image obtained from the satellite pass indicated in the right panel. It can be seen that the electron density in the F2 layer has only weak spatial structure, with no clear steep horizontal gradients. There is a localised region with enhanced densities between about 73^{0}N and 77^{0}N, with weaker isolated structures to the north. The red arrows mark the north-south limits of the NIMS intersection with the 630.0 nm activities. There is close agreement between the location of the structured F2 density enhancements and the red-line optical emissions. It can be noted that a weak positive density gradient exists between about 73^{0}N and 75^{0}N, in the vicinity of the equatorward limits of both the cusp auroral emissions and the regions of broad spectral width backscatter in the NIMS sector. The electron density peaks at about 2.0x10^{11} m^{-3} at ~75.0^{0}N and 320 km altitude.

The linear growth rate of the gradient drift process which can be calculated from the plasma drift relative to the neutral gass and the gradient drift scale length is given by the following formula (Tsunoda, 1988):

$$T = \left[\frac{1}{n_0} \frac{\Delta n}{\Delta x} \frac{E}{B} \right]^{-1} \qquad \text{(Eq. 1)}$$

where n_o is the background density and $\Delta n / \Delta x$ is the northward density gradient across the cusp boundary, and the E / B is the convection speed normal to the convection boundary.

For the case presented in Figure 3, at 320 km altitude the electron density increases from n_o = ~1.5 x10^{11} m^{-3} at 73.5^{0}N, to 2.0 x10^{11} m^{-3} at 75^{0}N, i.e. $\Delta n / \Delta x$ = ~0.5 x10^{11} m^{-3} / 165 x 10^3 m. The boundary normal speed measured by CUTLASS was 800 ms^{-1}. Plugging in these numbers in Eq. 1 gives a linear growth time of 10 minutes. However, it must be noted that the tomographic technique requires observations to be made for a range of ray-path geometries over a period of several minutes. The resultant integration effect in a poleward convecting flow will act to smooth out the density gradient to some degree, so that the estimated growth time could be an overestimate by possibly up to an order of magnitude. Nevertheless, this example suggests that the order of minutes would be needed for the irregularities to develop, during which time the prevailing convection would have carried the ionisation poleward hundred of kilometres. Hence a clear spatial separation would be expected between the onset of backscatter and the boundary of the cusp auroral emissions. No such division can be seen in Figure 3, so that the operation of the gradient-drift mechanism alone on the large-scale gradient seems inadequate to explain the observations using the experimental data at hand.

The collocation in latitude of the onsets of the small-scale irregularities responsible for backscatter and the optical emissions is most easily explained if both have a common source. Red-line cusp auroras arise from precipitation of low-energy magnetosheath particles that also cause enhancements in electron density at F-layer altitudes. Backscattering of the radar signals arises from irregularities transverse to the magnetic field at the Bragg scale, which is about 15 m for the current observations. It is possible that the precipitation is itself spatially structured on a sufficiently small scale to be responsible for the irregularities causing the

backscatter. There is evidence of finer structure in the cusp region than the large-scale gradient imaged here. For example, Huber and Sofko (2000) describe observations of double-peaked HF radar spectra that were interpreted in terms of vortices of scale less than 25km and lifetimes of 4s. Soterelis and Newell (2000) showed evidence of structuring in the primary cusp electrons at a resolution of 1s of DMSP satellite motion or 7km in space. The cusp region is also known to be a turbulent plasma rich in wave activity. Andrè et al (2000) used the action of Pc-1 and Pc-2 waves to explain the broadening of HF Doppler spectra and it is possible that such waves may play a role in the generation of decameter-scale irregularities. It is thus possible that the large-scale gradient measured in the present case contains steep sub-structures that are unstable in the poleward flow, generating irregularities that themselves cascade to spawn backscatter targets. With growth times inversely related to gradient scale lengths it is possible the the entire process may be completed on a spatial scale comparable to the uncertainties and the resolution limits of the current measurements, which are of the order of several tens of kilometres for each of the three techniques. It is thus not possible to differentiate between mechanisms related to decametre structure in the primary electron precipitation or gradient-drift instability and cascade from intermediate scale features on the basis of the present observation. Indeed, it must be noted that the field-aligned currents in the cusp might also make the current-convective instability another candidate process.

Figure 3 shows that radar returns were also observed at ranges far to the north of the band of aurora in a region where the large-scale gradient in the tomographic image would suggest stabilization of the plasma. It is possible that those signals result from irregularities formed in the auroral band and subsequently convected poleward out of the source region. However, decametre-scale irregularities have rapid decay times of durations of seconds, so that radar backscatter is found only in regions close to the source of the structures (e.g. *Tsunoda*, 1988). Thus in the present case, some source mechanism must be operating to create small-scale features in the plasma well to the north of the band of optical aurora. It has already been noted that the precipitation contains a wide spectrum of spatial scales, so that the turbulent plasma will have steep gradients on many different scales. The gradient-drift mechanism will continue to operate on these intermediate size structures, causing breakdown to the metre-scale lengths responsible for the backscatter. In the power law environment of the turbulent irregularity field, the magnitude of the perturbations is scale dependent, so that irregularities of increasingly larger scales will survive longer as they are carried from the source region. However, unstable gradients within these larger scales continue to spawn smaller structures, so that backscatter continues to be detected far to the north of the band of auroral precipitation as the flux tubes convect out of the cusp into the mantle.

3.3 Summary and Conclusions

1. The spectral width criterion of ≥ 220 ms^{-1} proves to be a robust cusp discriminator.

2. The equatorward edge of the optical cusp lines up with the equatorward edge of the HF radar cusp defined by the spectral width criterion ≥ 220 ms^{-1}.

3. We have not been able to single out the dominant mechanism for generating cusp irregularities.

A next step will be to combine the type of studies described in this report with data obtained from the scintillation receivers on Svalbard, and see if there is a relationship between

decameter irregularities and irregularities on the order hundred meters to kilometer scale size. We would like to emphasize that the outcome of this research may have practical relevance for transmission of satellite signals through the ionosphere. Under certain geophysical conditions obscuration of GPS signals does occur near the edges of the auroral oval, likely due to density gradients and plasma irregularities.

4. References

André, R., C. Hanuise, J.-P. Villain, and J.-C. Cerisier, HF radars: multifrequency study of refraction effects and localization of scattering, *Radio Sci., 32*, 153, 1997.

André, R., M. Pinnock, and A. S. Rodger, On the SuperDARN autocorrelation function observed in the ionospheric cusp, *Geophys. Res. Lett., 26*, 3353, 1999.

Basu, S., Su. Basu, P. K. Chaturvedi, C. M. Bryant, Jr, Irregularity structures in the cusp/cleft and polar cap regions, *Radio Sci., 29*, 195, 1994.

Huber, M., and G. J. Sofko, Small-scale vortices in the high-latitude F region, 105, 20885-20897, 2000.

Milan, S. E., M. Lester, S. W. H. Cowley, J. Moen, P. E. Sandholt, and C. J. Owen, Meridian-scanning photometer, coherent HF radar, and magnetometer observations of the cusp: a case study, *Ann. Geophysicae, 17*, 159, 1999.

Moen, J., D. Evans, H. C. Carlson, and M. Lockwood, Dayside moving auroral transients related to LLBL dynamics, *Geophys. Res. Lett., 23*, 3247, 1996.

Moen, J., D. A. Lorentzen, F. Sigernes, Dayside moving auroral forms and bursty proton auroral events in relation to particle boundaries observed by NOAA-12, *J. Geophys. Res., 103*, 14855, 1998.

Moen, J., H. C. Carlson, and P. E. Sandholt, Continuous Observation of Cusp Auroral Dynamics in Response to an IMF B_Y Polarity Change, *Geophys. Res. Lett., 26*, 1243, 1999.

Moen, J., H. C. Carlson, S. Milan, N. Shumilov, B. Lybekk, P. E.Sandholt, and M. Lester, On the collocation between dayside auroral activity and coherent HF backscatter,, *Ann. Geophysicae, 18,* 1531-1549, 2001.

Moen, J., I. K. Walker, L. Kersley, and S. E. Milan, On the generation of cusp HF-backscatter irregularities, *J. Geophys. Res..*, in press, April 2002.

Newell, P.T., and C.-I. Meng, The cusp and the cleft/boundary layer: low-altitude identification and statistical local time variation, *J. Geophys. Res., 93*, 14549, 1988.

Ossakow, S. L., and P. K. Chaturverdi, Current convective instability in the diffuse aurora, *Geophys. Res. Lett., 6*, 332, 1979.

Rodger, A. S., S. B. Mende, T. J. Rosenberg, and K. B. Baker, Simultaneous optical and HF radar observations of the ionospheric cusp, *Geophys. Res. Lett., 22*, 2045, 1995.

Sandholt, P.E., J. Moen, A. Rudland, D. Opsvik, W.F. Denig, and T. Hansen, Auroral event sequences at the dayside polar cap boundary for positive and negative IMF B_Y, *J. Geophys. Res., 98*, 7737, 1993.

Sandholt, P.E., C.J. Farrugia, J. Moen, Ø. Noraberg, B. Lybekk, T. Sten, and T.L. Hansen, A classification of dayside auroral forms and activities as a function of IMF orientation, *J. Geophys. Res., 103*, 23325, 1998.

Sotirelis, T., and P. T. Newell, Boundary-oriented electron precipitation model, *J. Geophys. Res*., 105, 18655-18673, 2000.

Tsunuda, R. T., High-latitude F-region irregularities: A review and synthesis, *Rev. Geophys., 26*, 719, 1988.

Villain, J. P., G. Caudal, and C. Hanuise, A SAFARI-EISCAT comparison between the velocity of F region small-scale irregularities and the ion drift, *J. Geophys. Res., 90*, 8433, 1985.

Wright, D.M. and T.K. Yeoman, High resolution bistatic HF radar observations of ULF waves in artificially generated backscatter, *Geophys. Res. Lett., 26*, 2825, 1999.

Yeoman, T. K., M. Lester, S. W. H. Cowley, S. E. Milan, J. Moen and P. E. Sandholt, Simultaneous observations of the cusp in optical, DMSP and HF radar data, *Geophys. Res. Lett., 24*, 2251, 1997.

APPENDIX A

PCIP campaign 15-21 December, 2001

Core instrumentation:
Ny-Ålesund (NYA): All-sky Imager (UiO), MSP (UiO), All-sky Imager (AFRL)

Longyearbyen (LYR) : ESR-1, MSP (U.Alaska)

Tromsø (TRO): UHF and VHF

+ CUTLASS HF

Participating people:
Lybekk, Basu, Ning, Kuenzler (NYA); Carlson, Moen, Nielsen, Oksavik, Shumilov (LYR); Paul Gallop (TRO)

EISCAT Mode descriptions:
30 sec dwell and 10 sec motion (first 10 s of every 40 s is moving)
Mode A: El 21.5; Az 7.5, 15, 22.5, 30, 22.5, 15, 22.5, 15 (2 min half cycle)
Mode B: El 21.5; Az 330, 337.5, 345, 352.5, 360, 7.5, 15, 7.5, 360, 352.5, 345, 337.5 (4 min half cycle)
Mode C: El 21.5; Az 337.5, 345.5, 352.5, 360, 352.5, 345 (2 min half cycle)
Mode D: Az 360; El 21.5, 23.5, 21.5, 25.5, 21.5
Mode E: Az 315, 322.5, 330, 337.5, 330, 322.5 (2 min half cycle)

ESR-1 Mode descriptions:

Mode 01-90 E: El 30; Az 15-105 (128s half cycle)
Mode 03-90 W: El 150; Az 15-105 (128s half cycle)
Mode 04-90 N: El 30; Az (-75)-15 (128s half cycle)
Mode 05-90 S: El 30; Az 105-195 (128s half cycle)
Mode 06-120 E: El 30; Az 0-120 (192s half cycle)
Mode 07-120 W: El 150; Az 0-120 (192s half cycle)
Mode 08-120 N: El 30; Az (-60)-60 (192s half cycle)
Mode 09-120 S: El 30; Az 90-210 (192s half cycle)
Mode 10-360 N: El 150; Az (-225)-135 (512s half cycle)
Mode 11-120 N + vertical (ESR-2): El 30; Az (-60)-60 (384s half cycle)

Day/time	**ESR-1**	**VHF**	**UHF**	**CUTLASS**	**Optics + other comments**
15.12.01/					Cloudy – wind from south west and snow showers
06:00	Mode 06-120E	Looking up, Then low el. north as it should	Mode A	Some backscatter far into the polar cap	IMF dominated by By positive, Bz increasingly negative. Polar cap potential increasing from 30-70 kV
07:00					IMF Bz dominated, By predominantly positive, convection pattern getting more symmetric, LYR MSP locates auroras through the cloud cover. Intense

					pulses of H_β aurora
07:46.23	Stop Mode 06-120E				
07:46.50	Start Mode 02-MSP		Mode B	Strong echoes above Svalbard	~07:50-08:20 Bz fluctuated between -8 to +2 nT
08:00	High Te, particle prec			Strong echoes above Svalbard	Disordered flow
08:20					Steadily westward flow
08:50					Optical recording from NYA starts
09:08.00	Stop Mode 02-MSP				
09:08.20	Start Mode 06-120E		Mode A		Look east-ward again to view the cusp/patch formation region
09:27.41	Stop Mode 06-120E		Mode C		Cusp on the west-side
09:28	Start Mode 07-120W				
11:00	Stop	Stop	Stop	Good HF backscatter	Completely overcast
16.12.01/					Cloudy at NYA and LYR – No optics. High densities in the solar wind (10-20 cm^{-3}) and solar wind speed of 500 kms^{-1}
06:00	Start Mode 08-120N	Start	Mode B	Good HF backscatter	Lobe reconnection, Bz (+), By (-)
06:30.25	Stop Mode 08-120N				
06:30.49	Start Mode 06-120E Problems with tel-connect/ radar drop out		Mode A	Good HF backscatter	Cusp over to the east, Bz (-), By small positive.
08:19.39	Stop Mode 06-120E				
08:20.09	Start Mode 08-120N		Mode B	Good HF backscatter	By (+) dominated, stirring lobe cell
08:56			Mode E	Good HF backscatter	Nice flow shear, with density structure. Protons probably cause E-region ionisation. **Start seeing aurora through at NYA**

09:30.40	Stop Mode 08-120N				
09:31.31	Start Mode 07-120W				Strong west-ward flows, Bz (-) and By (+) dominated fantastic H_α
11:00	Stop	Stop	Stop	Good backscatter	
17.12.01/					Clear skies at NYA and LYR. Normal densities in the solar wind and solar wind speed of 450-500 kms^{-1}
06:00	Start Mode 06-120E	Start	Antenna not moving	Poor backscatter	Aurora in south-east. IMF Bz (-) and By (+)
06:35	Airport interlock			Finland sees backscatter	
06:50	Start Mode 02-MSP				
07:00	Airport interlock				
07:14.49	Start Mode 02-MSP			Good Finland backscatter	Poleward moving forms, Cutlass sees the flow shear
07:33	Airport interlock			Good Finland backscatter	
07:45.39	Back on				
09:20			Mode B	Poorer backscatter	
09:30					IMF due south, poleward moving forms
09:57.07	Stop Mode 02-MSP		Mode C		
09:57.51	Start Mode 07-120W				
11:00	Stop	Stop	Stop	No backscatter	Active aurora, more green dominated
18.12.01					Clear skies at NYA and LYR. Normal densities in the solar wind and solar wind speed of 450-500 kms^{-1}
03:01.11	El 30, Az 215	Start	UHF won't move in elevation		Interesting flow reversal identified by ESR

03:50			Mode C		Predominantly westward flow
04:45			Problem with the UHF receiver, strange Doppler shifts	No backscatter	Probably no UHF data
05:15				Some backscatter	
05:50				Some backscatter	IMF Bz response in the return flow
06:29	Stop fixed mode				
06:31	Start Mode 06-120E			Good backscatter	IMF Bz(-) and By(+)
08:07	Stop Mode 06-120E				
08:07.54	Start Mode 02-MSP			Good backscatter	Poleward moving forms
	Airport interlock				
08:18.00	Start again			Good backscatter	Cusp aurora
08:25			Mode A starts	Good backscatter	Cusp aurora
08:32			Mode B	Good backscatter	Cusp aurora
08:22.35	Stop Mode 02-MSP			Good backscatter	Cusp aurora
08:23.04	Start Mode 07-120W			Good backscatter	Cusp aurora
09:28			Mode C	Good backscatter	Cusp aurora
09:54			Mode E	Good backscatter	Cusp aurora
10:31.57	Airport interlock			Good backscatter	Cusp aurora
10:45	Mode 10-360				
11:00	Stop	Stop	Stop		
19.12.01					Clear sky at LYR, some clouds at Ny-Ålesund, in particular at the northern sky. Normal densities in the solar wind and solar wind speed of 450 kms^{-1}
06:00	Start Mode 06-120E	Start	Mode A		IMF Bz (-), By fluctuating

07:00		Stop/ problems			
07:30					Brief northward turning in IMF
08:21.08				HF backscatter NW	
08:22	Start Mode 07-120W		Mode E		
08:48	Stop Mode 07-120W			Good HF backscatter	
08:48.35	Start Mode 02-MSP				
09:05			Mode B		
10:55	Stop	Stop	Stop	Patchy backscatter	
20.12.01					Overcast at LYR, clear sky and nice auroras at Ny-Ålesund, solar wind speed about 400 kms^{-1}
06:00	Start Mode 06-120E	Technical problems	Technical problems	Finland and Iceland backscatter	IMF Bz (-), By (+)
07:45		Start	Mode A		
07:25-35	Airport interlock				
08:01.56	Stop Mode 06-120 E			Good Finland backscatter	
08:02.07	Start Mode 02-MSP		Mode B		
09:00					IMF Bz (-), By small
10:06	Stop Mode 02-MSP		Mode E		
10:06.50	Start Mode 07-120W			Finland and Iceland	
11:00	Stop	Stop	Stop		

APPENDIX B

```
##########################################################
#                                                        #
#          OPTICAL OBSERVATIONS OF THE AURORA            #
#               IN NY AALESUND                           #
#                 SVALBARD                               #
#              JANUARY 2002                              #
#                                                        #
##########################################################
```

Instruments:
- US Camera
- UiO MSP (Meridian Scanning Photometer, MSP)
- UiO Camera
- Unis Spectrometer

Wednesday 9 January 2002 :
==========

Arrived in Ny Aalesund after two days delay. Due to bad weather the plain did not leave from Tromsoe on Monday and there was no conditions for the Longyear-Ny Aalesund flight on Tuesday.

Clouds in Ny Aalesund all day.

Thursday 10 January 2002 :
==========

05:00 UT Mostly clear sky.
05:25 UT Starts the MSP.
Did not find the 110V in the observation room. Connected the cameras to the 220->100V transformer.
05:40 UT Start the US Camera
05:59 UT Lots of stars visible, 1/8 cloud coverage
05:58 UT Starts the UiO Camera, arc in zenith
06:30 UT More clouds, only two stars visible, stop the US Camera
07:50 UT Stop UiO Camera and UiO MSP
08:59 UT Clouds all over, no wind, -11.3 deg, C
11:00 UT Clouds
Help from NP to reset the 110V fuse, then OK.
Calibrate the MSP the rest of the day.
16:45 Start the UiO Camera, Aurora at southern hemisphere
17:45 Overcast again, stop UiO Camera

Friday 11 January 2002:
==========

05:00 Snow, drifting snow and wind
Overcast and bad weather all day, no optical observations.
Compute the MSP calibrations.

Saturday 12 January 2002:
==========

04:00, 05:00, 07:00, 10:00 UT Clouds, clouds all morning
Continue computing the MSP calibration.
17:12 UT Many stars are visible, start the MSP, no aurora.
17:35 UT Start the UiO Camera, 2/8 cloud coverage

17:40 UT Start the US Camera.
19:48 UT Clear sky, some clouds at northern horizon
21:07 UT Bright clear sky, aurora in south, all instruments are running
22:02 - 22:15 UT Runs UiO Camera without filter in order to compare with the xephem star map.
22:20 UT Mostly clear sky

Sunday 13 January 2002:
=======================
05:00 UT Clouds all over, stop all instruments
07:00, 09:00, 10:00, 13:00 Clouds, clouds all morning
16;00 UT Mostly clear sky, start MSP, UiO camera and US camera
16:07 UT Clear sky all over
17:38 UT Mostly clear sky
19:00, 20:50 UT Mostly clear sky, aurora in south
20:30 UT Some more clouds, many stars visible
21:16 UT Clear sky, all instruments are running, no aurora

Monday 14 January 2002:
=======================
01:00 UT Some stars visible
05:00 UT Clear sky
05:30 UT Clear sky, lots of aurora south of zenith
05:39 UT Clear sky, arc/corona in zenith
06:36 UT Clear sky but some haze
07:16, 07:40 UT Clear sky
08:40 UT some more clouds, but still a lot of stars visible
09:00 UT US Camera stopped automatically as written in the schedule.txt file
51% of the harddisk space is used.
09:20 UT Some more clouds now but the instruments can see the cusp trough the clouds
09:52 UT Thin clouds, the cusp is still visible trough the clouds
Install the Unis spectrometer the rest of the day.
Clouds the rest of the day.

Tuesday 15 January 2002:
========================
05:00 UT Clear sky
05:28 UT Start MSP, and UiO camera, faint aurora in the south
05:40 UT Start US Camera
06:10 UT Clear sky, corona on southern hemisphere
06:45 UT Clear sky, corona in zenith
07:30 UT Clear sky, cusp at 115 deg elevation
08:27 UT Clear sky, aurora all over
08:53 UT US Camera automatically stopped
09:40 UT Stop UiO camera, install spectrometer
11:10 UT Clouds, stop the MSP
14:16 UT Clear sky start MSP
Working with the Unis spectrometer
18:00 UT Start the UiO camera
18:15 UT Start the US camera, aurora in the south
19:00, 19:15, 19:30, 20:20 UT Clear sky, aurora in the south, all instruments are running

Wednesday 16 Jan 2002:
======================
05:00 UT Clouds, snowing
05:15 UT Shuts down cameras and MSP
06:30, 07:30 UT Clouds and snow
Overcast the rest of the morning
17:10 UT Start to clear up, starts the MSP
18:20 UT Start the UiO camera

18:25 UT Start the US camera
Nice clear sky the rest of the evening

Thursday 17 Jan 2002:
==========
05:00 UT Clear sky, all instruments are running
06:15 UT Clear sky, arcs in zenith
07:00 UT Clear sky
07:45 UT Clear sky, lots of aurora, lights on airport runway is on
08:36 UT US Camera automatically stopped.
The harddisk on the US Camera PC was 97% full . Removed this harddisk and installed the second empty one.
11:00 UT Clear sky, cusp in zenith
13:00, 14:00 UT Nice clear sky, arc south of zenith
Nice clear sky the rest of the evening
19:00 UT Absolutely clear sky
20:30 UT Clear sky, increasing aurora in the south

Friday 18 Jan 2002:
==========
01:39 UT Clear sky, no aurora, all instruments are running
The harddisk on the US Camera PC was 10% full
02:00 UT Cluster satellite pass. Clear sky and faint 630.0 nm aurora in the east.
02:18 UT More aurora arrives
02:22 UT Arc in north at 22 deg. elevation
02:24 UT Some type of theta aurora, clear sky ?
06:00, 06:30, 07:25 UT Clear sky
08:13 UT Thin haze but still many stars are visible, corona in zenith
08:50, 09:30, 10:00, 11:58 UT Clear sky
11:58 UT Cluster satellite pass, aurora in zenith
12:00, 13:00, 14:00 UT Clear sky
15:00 UT Clear sky, some haze in south-west
17:00 UT Clear sky, aurora in south
18:00 UT Clear sky, aurora in east
19:00 UT Clear sky
19:02:50 UT Planet in MSP scan HB and 4278 channel (Jupiter ?)
20:08 UT Clear sky, very faint 630.0 nm

Saturday 19 Jan 2002:
==========
Clear sky in the early morning.
07:09 UT Clear sky, faint broad cusp north of zenith
630.0 nm emission north of zenith and 557.7 nm emission south of zenith
07:30, 08:00, 08:20 UT Clear sky, cusp in north
08:30 UT US Camera automatically stopped.
09:00, 09:30, 10:45, 11:30 Clear sky, aurora north of zenith
11:45 UT Some more clouds in north
11:48 UT Increasing activity
13:00 UT Some haze, but still some stars are visible
15:46 UT Arc in zenith, some haze
17:00 UT Some haze, clouds in North and West, faint arc in zenith
18:40 UT Clouds stop UiO camera and MSP
Clouds the rest of the evening.

Sunday 20 Jan 2002:
==========
05:00 UT Clear sky, some clouds in north
05:25 UT Start MSP and UiO camera
05:35 UT Start US camera
06:00 UT Clear sky, some clouds at horizon in south and east

06:44 UT Thicker clouds, only three stars are visible
07:22 UT To much clouds, stop both cameras and the MSP
       Clouds the rest of the day.
       Replaced the UiO camera PC 75GB datadisk
         E:\data\images is the location of the images.
22:50 UT Clear sky again, lots of aurora
       Start UiO camera, US camera and the MSP
       Clear sky all night

Monday 21 Jan 2002:
==========
06:25 UT Clear sky, lots of aurora overhead
06:46, 07:20, 08:15 UT Clear sky, aurora in zenith
08:18 UT US Camera automatically stopped.
09:10 UT To much sunlight for MSP, stop the instrument
09:23 UT Stop UiO Camera

Power down all instruments:
 - US camera, US camera controller, US camera PC
 - UiO camera, UiO camera controller, UiO camera PC
 - MSP PC, (MSP instrument is on).
 - Unis Spectrometer (see Unis Spectrometer manual)
       unplugged all power to Unis Spectrometer.
       (Unis Spectrometer PC is on)
 - Stopped heater to camera dome.
 - Stopped heater to spectrometer dome.
 - Put cover on MSP box

Leave Ny Aalesund, end of this observation period

Bjoern Lybekk
Department of Physics
University of Oslo

APPENDIX C

PCFL campaign 6-10 January, 2002

Core instrumentation:
Ny-Ålesund (NYA): All-sky Imager (UiO), MSP (UiO), All-sky Imager (AFRL)

Longyearbyen (LYR): ESR-1, MSP (U.Alaska)

Tromsø (TRO): UHF and VHF

+ CUTLASS HF

Participating people:
Ning (NYA); Carlson, Moen, Oksavik, Shumilov (LYR); Paul Gallop (TRO)

EISCAT Mode descriptions:
30 sec dwell and 10 sec motion (first 10 s of every 40 s is moving)
Mode West: A: El 21.5; Az 330, 315, 300, 285, 300, 315 (4 min cycle)
Mode East: El 21.5; Az 15, 30, 45, 60, 45, 30 (3/4 min cycle)

ESR-1 Mode descriptions:

Mode East: El. 30: Az (-30)-160 windshield (3minutes-192 s/ 4 minutes-256s)
Mode West: El. 150: Az (-30)-160 windshield (3minutes-192 s/ 4 minutes-256s)
Mode North: El. 30: Az (-90)-90 windshield (3 minutes -192 s)
Mode 4 from Jan 2001: az = [-75,15], el = 30 (P = 2 min (256s) cycle time)

Day/time	**ESR-1**	**VHF**	**UHF**	**CUTLASS**	**Optics + other comments**
06.02.02					Clear skies at NYA and LYR. Normal densities in the solar wind and solar wind speed of 600-650 kms^{-1}
16:01.10	El=30, Az=[-30,160] 256s				
16:23		Start			Arc at LYR zenith, 10 min life time
17:00	Interlock due to snow				
17:36	El=30, Az=[-30,160] 192s				
17:40			Mode East		
18:30				Good backscatter	Negative Bay H-comp
19:30					Poleward leap, equatorward moving forms
20:10					Very active
20:20				Good backscatter	Brightening in south again
20:50					Curls/folds southward drifting
21:11	El=150,Az=[-30,160] 192s		Mode West		
21:30				Good backscatter	Response to an IMF south/ 15 minutes
22:20					Sun-aligned arc
23:00	Stop	Stop	Stop		

07.02.02					
16:00		Start	Mode East –weak signal from the UHF		No internet connection and therefore start problems on the radar. Polar cap contracted, 25 kV according to the APL-model, arc above zenith at NYA, clear skies at NYA and LYR
17:15	El=30, Az = [-75,15] 128s		bits		IMF Bz predominantly poleward
17:50	Stop		and		
18:05	El=30, Az=[-90,90] 192s		pieces	Good backscatter	Very high electron densities seen by ESR
19:00					See a strong flow shear, high densities, auroral intensification at the southern horizon seen from NYA
19:38					Two negative cells under Bx negative!!
19:48			UHF data start getting reliable		PATCHES!
20:05			Mode East stop		
20:05			Az +15 fixed		
20:20					Substorm onset above North-Norway
20:30					IMF Bz south
20:50					Sun-aligned arc –maybe associated with a reversal in By (-/+)
21:04.25	Stop				
21:04.25	El=30,Az = [-80,140] 256s				
22:00					IMF Bx negative dominance
23:00	Stop	Stop	Stop		

08.02.02					
16:00	El=30,Az = [-30,160] 192s	Start	Az +15 fixed		IMF Bz south, partly cloudy but OK at LYR, overcast at NYA
16:30					Strong aurora above the radar, 300 nT negative bay in the H-component
17:00					Clear sky at Ny-Ålesund
17:30					Partly cloudy at NYA
18:00				Good cutlass backscatter	Strong electron densities
19:40					IMF dominated by Bx-negative, two negative cells
20:25					Clear at NYA again – stars and patches
20:30					Patches above Ny-Ålesund
21:28.25	El=30,Az = [-130,160] 256s				
23:00	Stop	Stop	Stop		
09.02.02					Clear skies at NYA and LYR. Normal densities in the solar wind and solar wind speed of 450 kms^{-1}, Bz-component
16:00	El=30,Az = [-30,160] 192s	Start	Az +15 fixed	Good CUTLASS backscatter	
17:15					Arc above Ny-Ålesund, quite magnetic conditions
17:57	El=30,Az = [-120,160] 256s				
19:04					Nice arc above NYA-sun-aligned?
19:24					Strong activity above Svalbard

20:00	5 min off the air				Arc in due south
20:15	El=30,Az = [-120,160] 384				Eastern part of the all-sky image dark
20:10					Substorm onset – pulled in dense plasma on the nightside
21:26			Stop		
21:30					Poleward expansion
21:53			Start Az + 315		
22:00	Stop	Stop	Stop		